J. Phycol. **49,** 502–516 (2013)

DOI: 10.1111/jpy.12057

MEASURING CARBON AND N_2 FIXATION IN FIELD POPULATIONS OF COLONIAL AND FREE-LIVING UNICELLULAR CYANOBACTERIA USING NANOMETER-SCALE SECONDARY ION MASS SPECTROMETRY[1]

Rachel A. Foster,[2] *Saar Sztejrenszus,*[3] *and Marcel M. M. Kuypers*

Department of Biogeochemistry, Max Planck Institute for Marine Microbiology, Celsiusstr 1, Bremen D-28359, Germany

Unicellular cyanobacteria are now recognized as important to the marine N and C cycles in open ocean gyres, yet there are few direct *in situ* measurements of their activities. Using a high-resolution nanometer scale secondary ion mass spectrometer (nanoSIMS), single cell N_2 and C fixation rates were estimated for unicellular cyanobacteria resembling N_2 fixer *Crocosphaera watsonii*. *Crocosphaera watsonii*-like cells were observed in the subtropical North Pacific gyre (22°45′ N, 158°0′ W) as 2 different phenotypes: colonial and free-living. Colonies containing 3–242 cells per colony were observed and cell density in colonies increased with incubation time. Estimated C fixation rates were similarly high in both phenotypes and unexpectedly for unicellular cyanobacteria 85% of the colonial cells incubated during midday were also enriched in ^{15}N above natural abundance. Highest ^{15}N enrichment and N_2 fixation rates were found in cells incubated overnight where up to 64% of the total daily fixed N in the upper surface waters was attributed to both phenotypes. The colonial cells retained newly fixed C in a sulfur-rich matrix surrounding the cells and often cells of both phenotypes possessed areas (<1 nm) of enriched ^{15}N and ^{13}C resembling storage granules. The nanoSIMS imaging of the colonial cells also showed evidence for a division of N_2 and C fixation activity across the colony where few individual cells (<34%) in a given colony were enriched in both ^{15}N and ^{13}C above the colony average. Our results provide new insights into the ecophysiology of unicellular cyanobacteria.

***Key index words:* *Crocosphaera*; diazocyte; N_2 fixation; nanoSIMS; unicellular**

Nitrogen fixation, or the reduction of di-nitrogen (N_2) gas to bio-available ammonium is an important new source of nitrogen (N) in the World's oceans (Karl et al. 1997, Capone et al. 2005), and is only catalyzed by a small number but broad diversity of microorganisms (Zehr et al. 1998). In the open ocean, cyanobacteria are one of the dominant N_2-fixing (diazotroph) groups of organisms where abundances of several lineages, including filamentous and unicellular types, often co-occur. The larger filamentous and symbiotic types (i.e., *Trichodesmium* spp. and *Richelia intracellularis*) have long been considered the primary N_2 fixers in open ocean gyres (Mague et al. 1974, Capone et al. 1997, Karl et al. 2002). However, more recently, unicellular cyanobacteria are now thought of as an equally important new source of N due to their high abundances and broad distributions (Needoba et al. 2007, Moisander et al. 2010). Further evidence for an important role of unicellular diazotrophic cyanobacteria is also provided by high N_2 fixation rates reported in the smaller size fractions (<10 μm) of bulk stable isotope ($^{15}N_2$) uptake experiments (Dore et al. 2002, Montoya et al. 2004, Zehr et al. 2007a, Grabowski et al. 2008, Bonnet et al. 2009, Kitajima et al. 2009, Sohm et al. 2011a), as well as results from recent modeling efforts (Goebel et al. 2007, Monteiro et al. 2010).

Three groups of marine N_2-fixing unicellular cyanobacteria, A, B, and C, can be distinguished based on their *nifH* gene sequence, which encodes for the nitrogenase enzyme for N_2 fixation (Zehr et al. 2001, Foster et al. 2007). More recently, the groups are referred to as UCYN-A, UCYN-B, and UCYN-C. UCYN-B is the only group with a cultured representative, *Crocosphaera watsonii* WH8501, which was isolated from the western tropical South Atlantic Ocean in the mid 1980s (Waterbury and Rippka 1989). Currently, there are up to 10 different strains of *C. watsonii* isolated from the open ocean (Atlantic and Pacific Oceans; Webb et al. 2009) which possess great phenotypic plasticity while maintaining high genetic conservation (Zehr et al. 2007b, Webb et al. 2009, Bench et al. 2011). The isolated strains of *Crocosphaera* can be distinguished based on cell diameter where the larger cell diameter (>4 μm) type strains produce substantial amounts of extracellular material (ECM) recently defined as an extracellular polysaccharide (EPS; Webb et al. 2009, Sohm et al. 2011b). The smaller cell diameter (<4.0 μm) strains also produce EPS, however, in lesser amounts (Webb et al. 2009, Sohm et al. 2011b). Field populations of *Crocosphaera*-like cells have also been observed forming loose groupings or colonies presumably held together by the EPS (Biegala and

[1]Received 6 August 2012. Accepted 5 February 2013.
[2]Author for correspondence: e-mail rfoster@mpi-bremen.de..
[3]Department of Microbial Ecophysiology, University of Bremen, Bremen D-28359, Germany
Editorial Responsibility: J. Raven (Associate Editor)

Raimbault 2008, Webb et al. 2009, Sohm et al. 2011b). The function of the EPS in *Crocosphaera* spp. is not known; however, other phytoplankton produce EPS as a carbon (C) reserve during nutrient limitation (Corzo et al. 2000), while in the unicellular diazotroph, *Cyanothece* spp., EPS has an acidic character, which may be beneficial for binding metals and the thick layering of EPS could potentially aid in oxygen protection (Reddy et al. 1996).

Since the nitrogenase enzyme is irreversibly inactivated by the presence of oxygen (Postgate 1998), N_2-fixing cyanobacteria have developed strategies to protect their nitrogenase enzyme from oxygen evolved during photosynthesis (Gallon and Chaplin 1988, Burris 1991, Fay 1992). In unicellular diazotrophic cyanobacteria, N_2 fixation is separated temporally to the night while photosynthesis occurs during the day (Griffiths et al. 1987, Fay 1992). Hence, the highest *nifH* transcription and N_2 fixation of *C. watsonii* and UCYN-B field populations are observed during the night (Tuit et al. 2004, Church et al. 2005a,b, Zehr et al. 2007a, Webb et al. 2009, Mohr et al. 2010a, Pennebaker et al. 2010, Shi et al. 2010, Saito et al. 2011). In heterocystous cyanobacteria, N_2 fixation is separated spatially into specialized thick-walled cells called heterocysts while photosynthesis occurs in vegetative cells (Wolk et al. 1976). A combination of both spatial and temporal separation can be found in the nonheterocystous colonial filamentous marine cyanobacterium, *Trichodesmium* spp., where N_2 fixation occurs during the day in only some of the cells along a filament (Bergman et al. 1997, Berman-Frank et al. 2001, Lundgren et al. 2001). The localized N_2-fixing cells are referred to as diazocytes. Others have shown in field and culture populations of *Trichodesmium* that in addition to a spatial separation, segregation of C and N_2 fixation can be influenced by temporal factors (Berman-Frank et al. 2001, Finzi-Hart et al. 2009). The colony formation in *Trichodesmium* and other cyanobacteria could therefore be strategic since physiological activities, e.g., photosynthesis and N_2 fixation, can occur simultaneously by partitioning the activity in time and space within the cells of a colony.

Recent methodological advancements in single cell technologies have made it possible to directly measure metabolic activities and variability of metabolic rates in individual cells (reviewed in Wagner 2009 and Musat et al. 2011). Here, we used a high-resolution nanometer scale secondary ion mass spectrometry (nanoSIMS) approach to directly measure individual carbon (C) and N_2 fixation rates of unicellular cyanobacterial cells from the subtropical North Pacific Gyre. The Hawaiian Ocean Time-series (HOT) field site was selected since it was easily accessible, oligotrophic, and a site where N_2 fixation has been previously measured and a variety of diazotrophic cyanobacteria are consistently observed throughout the year (Leteliar and Karl 1996, Karl et al. 1997, Dore et al. 2002, Falcon et al. 2004, Fong et al. 2008, Grabowski et al. 2008, Church et al. 2008, Sohm et al. 2011a).

In this study, we report single cell N_2 and C fixation rates for two phenotypic field populations of *C. watsonii*-like cells: free-living and colonial. Both phenotypes were present at the field site, and were amongst the more abundant diazotrophic cyanobacteria observed by microscopy. We initially hypothesized that the unicellular cyanobacterial cells living colonially could have an advantage similar to *Trichodesmium* spp. where N_2 fixation and photosynthesis could occur contemporaneously during the daytime. Although nanoSIMS imaging of both phenotypes of the *C. watsonii*-like cells showed an enrichment of ^{15}N after incubations during the day, our results are still speculative since other N_2 fixers were present and could contribute to a labeled and available dissolved inorganic nitrogen (DIN) pool. However, the nanoSIMS imaging did allow us to visualize a spatial heterogeneity of ^{15}N and ^{13}C across the colonies that suggested a division of metabolic activity amongst the cells. The results presented here provide new insights into the ecophysiology of two phenotypes of unicellular cyanobacteria common in the oligotrophic waters of the World's oceans.

MATERIALS AND METHODS

Water collection and incubation experiments. Whole seawater was collected during the HOT series cruise on 23–27 July 2009 (HOT-213) to station ALOHA (A Long-Term Oligotrophic Habitat Assessment; 22°45′ N, 158°0′ W) in the North Pacific subtropical gyre. Seawater samples were collected from Niskin bottles on 24 July 2009 from 15 m using a Conductivity Temperature Depth (CTD) rosette. Whole seawater was transferred directly into 12 acid rinsed 4.4 L light transparent polycarbonate bottles (Nalgene, Fisher Scientific, Pittsburgh, PA, USA). The bottles were filled without headspace and capped without air bubbles, and each bottle was amended with 1 mL of 0.2 M $NaH^{13}CO_3$ and 4 mL of 99 % $^{15}N_2$ (Cambridge Isotopes, Andover, MA, USA) through the septa cap (Thermo Fisher Scientific, Waltham, MA, USA) using gas tight syringes (Hamilton, Reno, NY, USA). The bottles were manually inverted for several minutes (5 min) to mix in the isotopes and placed on their sides in an on deck incubator provided by the ship (*R/V Kilo Moana*).

The bottles were incubated for ~0, 3.8, 12.3 and 18.3 h at ambient surface water temperatures (25.9°C) by continuously flowing surface seawater and shading to 50 % incident surface irradiance in the on deck incubator. Bottles were amended with isotopes between 11:30 and 11:40 and the sunset was ~19:10 and sunrise 6:00 (local time). Therefore, the latter two time points (12.3 and 18.3 h) were exposed to ~7.5 h of sunlight, and 4.8 and 10.8 h of darkness, respectively.

Nitrogen and carbon content and N_2 and C fixation rates of whole water incubations. At the time of injection (time 0), and at subsequent time points (3.8, 12.3 and 18.3 h), one of the 4.4 L incubation bottles was filtered using a peristaltic pump (Cole-Parmer, Vernon Hills, IL, USA) onto precombusted 25 mm diameter Glass Fiber Filter (GFF; GE

Healthcare Life Sciences, Pittsburgh, PA, USA) held within an acid-washed swinnex filter holder (Millipore, Billerca, MA, USA) and stored frozen (−20°C) until returned to the laboratory.

The GFFs were dried overnight at 60°C in an oven, acid fumed overnight in a desiccator with an open beaker of 37% hydrochloric acid (HCl) to remove inorganic C from the filters, and then placed again at 60°C for 1 h to complete dehydration. The dried filters were weighed and packed for combustion analysis. Both ^{15}N and ^{13}C (atom%) and the mass of the particulate organic carbon (C) and nitrogen (N;μg) were analyzed by an automated elemental analyser (Thermo Flash EA, 1112 Series) coupled to a Delta Plus Advantage isotope ratio mass spectrometer (Thermo Finnigan, Dreieich, Germany; EA-IRMS). Instrument accuracy and precision were estimated at 0.3652 ± 0.0001 ^{15}N atom% and 1.0664 ± 0.0006 ^{13}C atom% based on the mean and standard deviation of caffeine standards measured in conjunction with the samples. Fixation rates were calculated as a function of the change in the tracer concentration of the particulate organic pool relative to the size of the pool between time 0 and the 3 subsequent time points (3.8, 12.3 and 18.3 h) as described in detail elsewhere (Montoya et al. 1996).

NanoSIMS sampling. At the time of injection (time 0) and at the subsequent time points (3.8, 12.3, 18.3 h), a separate replicate 4.4 L bottle was filtered using the same peristaltic pump and swinnex filter holder described above onto a 3.0 μm pore size pre-sputtered gold (Au) palladium (Pd) 25 mm diameter membrane filter (Millipore). The cells on the Au-Pd sputtered filters were immediately fixed overnight in 100 μL of 4% paraformaldehyde (PFA; w:v) solution at 4°C, rinsed three times in 0.1 M phosphate buffered saline (PBS) and then stored dry at −20°C until further analysis. The 4% PFA solution was made up in 0.2 μm filtered seawater (FSW) collected from the same depth as collection (15 m) of the incubation water.

Microscopic identification, cell abundances, and marking for nanoSIMS. The Au-Pd sputtered filters were first scanned for unicellular cyanobacteria cells using a Zeiss Axioskop II fluorescence microscope (Zeiss, Berlin, Germany) fitted with blue (450–490 nm) and green (510–560 nm) excitation filters. Cyanobacterial cells were first identified by excitation patterns where cells were screened positive if a yellow-orange fluorescence (indicating the presence of chl *a*) was observed under blue excitation, and an orange-red fluorescence (indicating the presence of phycoerythrin) under green light excitation. Cells that displayed the appropriate excitation pattern were further identified as *C. watsonii*-like if the cell diameter was ~3–10 μm and the cells possessed a coccoid cell morphology.

Two independent methods, fluorescent in situ hybridization (FISH) and quantitative PCR (qPCR) on single cells with highly specific oligonucleotides, were unsuccessfully applied to verify the identity of the *C. watsonii*-like cells of our study. We concluded that the 4% PFA fixation step required for nanoSIMS interfered with the permeability of the cell membrane for FISH and the chemistry of the qPCR assay. To the best of our knowledge, *C. watsonii* WH8501 and some related strains (Webb et al. 2009) are the only unicellular N_2-fixing planktonic cyanobacteria with the above-mentioned characteristics common at station ALOHA, and therefore we assigned the cells of our study as *C. watsonii*-like.

The *C. watsonii*-like cells were further characterized into two phenotypes: (1) free-living if the cells were observed as single cells or (2) colonial if 3 or more cells were observed held in a matrix. It should be noted that the sampling, mixing, or filtration process could have influenced the formation of colonies. Cells that were observed as elongated or in the process of cellular division were also distinguished for both the free-living and colonial phenotypes. A third phenotype was identified as linear, where cells were observed connected in one long filament rather than as a cluster or colony of cells. The linear phenotype was only observed during the initial time point (time 0) and at the 3.8 h time point.

Microscopic counts were also performed with the Zeiss Axioskop II fluorescence microscope (Zeiss). On four select 3.0 Au-Pd pre-sputtered filters (time points: 0, 3.8, 12.3, and 18.3 h), *C. watsonii*-like cells were enumerated from 7 to 80 grids (grid area = 150062.5 μm^2), using the 20× objective. The grid areas were randomly selected. The number of grids depended on cell density such that at the later time points, more grids were counted to reach a statistically significant number of cells. The total number of cells per grid was 0–49 and 0–242 for the free-living and colonial phenotypes, respectively. A total of 3849 cells were enumerated (1123 free-living and 2726 colonial).

Prior to nanoSIMS analyses, 5 mm diameter sub-samples were excised from the Au-Pd filters, and areas containing colonies and free-living cells of *C. watsonii*-like cells were marked with arrows and numbers using a Laser Micro Dissection (LMD) microscope 6500 (Leica, Berlin, Germany). Microscopic pictures were taken and used for orientation purposes during subsequent nanoSIMS analysis and for post-processing using look@nanoSIMS software (see below). The charge-coupled device (CCD) camera on the nanoSIMS 50L instrument (Cameca, Gennevilliers, France) has limited resolution and therefore the laser markings allow the areas containing the target cells for analysis to be quickly re-identified.

NanoSIMS analysis and data processing. NanoSIMS analyses were performed using a Cameca NanoSIMS 50 L instrument (Cameca). Briefly, after identifying the laser marking with the CCD camera, samples were pre-sputtered for 1–2 min and rastered with 16 keV Cesium (Cs^+) primary ions with a current of between 1 and 3 pA. Primary ions were focused into nominal ~120 nm spot diameter. Mass resolving power in all measurements was >6000. The primary ion beam was used to raster the analyzed area (10 × 10 μm and 50 × 50 μm for the free-living cells and colonial cells, respectively) with 256 × 256 pixels over the chosen raster size with a dwelling time of 1 or 2 ms per pixel. Negative secondary ions ($^{12}C^-$, $^{13}C^-$, $^{12}C^{14}N^-$ $^{12}C^{15}N^-$, $^{32}S^-$) were collected simultaneously in electron multiplier detectors.

All scans (35–100 planes) were corrected for drift of the beam and sample stage after acquisition using the look@nanoSIMS software package (Polerecky et al. 2012). Isotope ratio image was created as ratio of a sum of counts for each pixel over all recorded planes of the investigated isotope and the main isotope. Regions of interest (ROI) were defined using secondary electron images, Total Ion Current (TIC), $^{12}C^{14}N$, and the epifluorescence microscope images taken prior to analysis. For each ROI, the isotopic ratio was calculated and corrected according to the mean isotopic value determined in the nanoSIMS analysis of 22 free-living and colonial cells from the initial time point (time 0). At the incubation time points (3.8, 12.3, 18.3 h), a total of 83–110 *C. watsonii*-like cells were analyzed with nanoSIMS, which was equivalent to 15 d ($8–10\ h \cdot d^{-1}$) of analysis (includes tuning).

Calculations: biovolume and biomass conversion, ^{13}C and ^{15}N assimilation, C-based growth rates, N and C contribution to whole water ^{13}C and ^{15}N assimilation. The cell diameter of individual *C. watonsii*-like cells was estimated from the nanoSIMS images after manually circling each cell using look@nanoSIMS software package (Polerecky et al. 2012). It should be noted that the cell diameter measurements could be underestimated

due to the fixation procedures in 4% PFA overnight required for the nanoSIMS analysis.

The biovolume (BV) was estimated using the equation for a sphere as reported in Sun and Liu (2003):

$$\mathrm{BV} = (\pi/6) \times \emptyset^3 \quad (1)$$

where Ø is the cell diameter. The initial carbon (C) content was estimated using the following relationship between BV and C content defined in Verity et al. (1992):

$$\mathrm{Log(C)} = -3.63 + 0.863(\mathrm{Log\ BV}) \quad (2)$$

Logarithms (LOG) are base 10 and the C content was then used to estimate N content by assuming a modified Redfield ratio (C:N) of 8.6 as reported by Tuit et al. (2004) for unicellular N_2-fixing cyanobacteria.

The cell-specific C and N_2 assimilation (F_C or F_N) was calculated for each time point as follows:

$$F_C = ({}^{13}C_{ex} \times C_{con})/C_{SR} \quad (3)$$

$$F_N = ({}^{15}N_{ex} \times N_{con})/N_{SR} \quad (4)$$

where $^{13}C_{ex}$ and $^{15}N_{ex}$ is the atom (AT) % of the $^{13}C/^{12}C$ and $^{15}N/^{14}N$, respectively, for a particular time point corrected for by the mean value of the respective ratios for cells analyzed in the time 0 samples. The C_{con} and N_{con} are the initial C and N content, respectively, estimated as described above in equation 2 and C_{SR} and N_{SR} are the labeling percentage of ^{13}C and ^{15}N, respectively, in the experimental bottle. The assimilated C and N were divided by the incubation time (h) to determine the cell-specific C and N_2 fixation rates. More details of calculations are described elsewhere (Montoya et al. 1996).

Growth rate was calculated by the following:

$$V = (1/t) \times (R_F - R_I)/(R_S - R_I) \quad (5)$$

where t is time in d, the R_F is estimated from the $^{13}C/^{12}C$ at a specific time point by the nanoSIMS, the R_I is the mean ^{13}C AT% of the cells from the time zero samples, and the R_S is the calculated labeling percentage of ^{13}C in the experimental bottle.

To estimate the contribution of the free-living and the colonial *C. watsonii*-like cells to the whole water (bulk) assimilation estimated by the EA-IRMS analyses, the bulk assimilation was divided by the mean N_2 and C assimilation from nanoSIMS analyses normalized to the cell abundances for the free-living and colonial cells (determined by the microscopy cell counts from each time point). It should be noted that the percent of active N_2-fixing cells was taken into account for the earlier time points (3.5 and 12.3 h) since not all cells were active for N_2 fixation.

In order to assess the spatial heterogeneity of the enrichment measured in the colonial cells, the mean value of $^{13}C/^{12}C$ and $^{15}N/^{14}N$ is calculated for the cells in a colony. Each time point had a certain number of colonies analyzed (8, 7, 9 colonies for 3.8, 12.3, and 18.3 time points, respectively) and the number of cells in a colony varied between 4 and 22 (Table S1, see Supporting Information). The cells in the colony were then counted, which were above the average for $^{13}C/^{12}C$, $^{15}N/^{14}N$, and for both ratios ($^{13}C/^{12}C$ and $^{15}N/^{14}N$). The values were then converted and reported as percentages.

RESULTS

Whole water measurements of N_2 and C fixation rates. Bottles containing whole water from a depth of 15 m were incubated in parallel to the bottles for nanoSIMS analysis in order to measure the whole community N_2 and C fixation rates (Table 1). The highest rates (33.7 nmol $C \cdot h^{-1} \cdot L^{-1}$) of bulk C fixation was measured during the first 3.8 h, which was also coincident with the highest daily irradiances. Similar trends were observed in the nanoSIMS analysis of single *C. watsonii*-like cells (see below). The $^{13}C/^{12}C$ ratio and estimated bulk C fixation rates decreased at the 12.3 h time point and in the bottle incubated overnight (18.3 h), indicating respiration of newly fixed C had occurred (Table 1). The N_2 fixation rates in the bulk bottles increased with incubation time such that the highest rates of N_2 fixation (1.88×10^{-2} nmol $N \cdot L^{-1} \cdot h^{-1}$) were estimated in the bottles incubated through the dark period, indicating that night N_2 fixation was greater than the daytime N_2 fixation (9.42×10^{-3} nmol $N \cdot L^{-1} \cdot h^{-1}$; Table 1).

Phenotypic characterization of C. watsonii*-like cells.* Both colonial and free-living *C. watsonii*-like cells were observed in our experiments. The colonial phenotype was more abundant at each time point and the number of cells per colony varied 3–243 cells (Table 1). The number of cells per colony observed increased during the incubation where at the time 0, 17 ± 7 cells per colony were noted, and at the final time point (18.3 h), the mean cells per colony was 33 ± 8 (Table 1). The pigmentation of the free-living phenotype was slightly different than that of the colonial cells. It was most noticeable in the field observations, where images taken under the same blue excitation filter shows the free-living cells with a slight orange hue, rather than the bright yellow observed in the colonial phenotype (Fig. 1, a and b).

During the first two time points (0 and 3.8 h), we observed 18 *C. watsonii*-like cells (12 and 6, respectively), which appeared as a linear filament, and these were treated as a separate phenotype (Table 2). The average cell diameter for the linear *C. watsonii*-like cells increased ~2-fold (3.73 ± 0.25–7.51 ± 0.38 μm) from the initial time point (time 0) to the 3.8 h time point. Subsequently at the later time points, the linear phenotype was not observed.

At each incubation time point, *C. watsonii*-like cells appearing elongated, connected, or in the process of cellular division were observed. It was particularly noticeable in the field observations of free-living cells made prior to setting up the incubation experiments (Fig. 1a) and in cells collected after the 3.8-h time point. The number of observations of dividing cells was higher in samples from the earlier time points (0 and 3.8 h) than in the samples collected at later time points (12.3 and 18.3 h; Table 2). Since the difference in cell

TABLE 1. Summary of microscopic cell counts of single and colonial *Crocosphaera watsonii*-like cells and the whole water C and N_2 fixation rates measured in the incubation experiments.

Date	Time (h)	Single cells · (L^{-1})	Colonial cells · (L^{-1})	Cells per colony range (mean SE)	N_2 fix rate (nmol N · L^{-1} · h^{-1})	C fix rate (Nmol C · L^{-1} · h^{-1})
24 July 2009	0	4.78×10^3	6.32×10^3	3–50 (17 ± 6.8)	n/a	n/a
24 July 2009	3.8	5.15×10^3	8.16×10^3	4–69 (19 ± 6)	9.41×10^{-3}	39.3
24 July 2009	12.3	6.33×10^3	1.01×10^4	3–242 (37 ± 10)	1.88×10^{-2}	13.1
25 July 2009	18.3	3.52×10^3	1.62×10^3	3–196 (33 ± 8)	1.42×10^{-2}	3.12

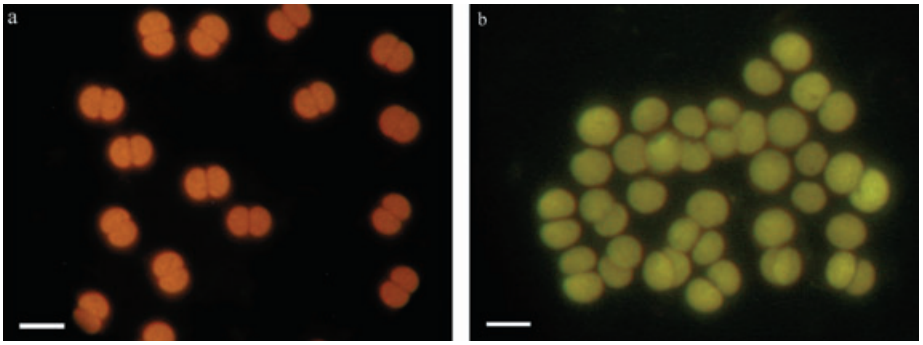

FIG. 1. Blue excitation epifluorescent micrographs of the two phenotypes of *Crocosphaera watsonii*-like cells imaged in the field at the time of the experiments. (a) The free-living phenotype shows many cells in the process of division. (b) The colonial phenotype. Scale bars are 5 μm.

diameter was usually significantly greater in the dividing cells for both the colonial and free-living phenotypes (*t*-test, $P < 0.05$), the cell diameter and enrichment ($^{13}C/^{12}C$ and $^{15}N/^{14}N$) data derived from dividing cells was not pooled for each respective phenotype (Table 2).

The average cell diameter for colonial *C. watsonii*-like cells was significantly larger in cells from the beginning of the experiment (time 0) and at two of the later time points (12.3 and 18.8 h) than the mean cell diameter for the free-living *C. watsonii*-like cells (*t*-test, $P < 0.001$). There was a gradual decline in the average cell diameter for the colonial *C. watsonii*-like cells during the incubation, whereas after an initial 1.5-fold increase in mean cell diameter from 4.32 to 6.46 μm, the free-living *C. watsonii*-like cells showed a similar decline in average cell diameter as the colonial *C. watsonii*-like cells (Table 2; Fig. 2, a and b).

Elemental composition of ECM excreted by colonial C. watsonii*-like cells.* Using nanoSIMS, we imaged the sulfur (^{32}S), carbon ($^{13}C/^{12}C$), and nitrogen ($^{15}N/^{14}N$) contents in the two different phenotypes of *C. watsonii*-like cells. The $^{32}S/^{12}C$ ratio of the material between the cells living colonially, herein referred to as ECM, was substantially higher than the cellular $^{32}S/^{12}C$ ratio (Fig. S1, see Supporting Information). A similar S-rich material was not observed surrounding the free-living cells. The ECM of the colonial cells was also highly enriched for ^{13}C and depleted in ^{15}N. It was most obvious in the colonial cells from the 3.8 h incubation time point (Fig. 3, b and d).

Single cell N_2 and C fixation rates, C:N ratios, and C- based growth rates of C. watsonii*-like cells.* The $^{15}N/^{14}N$ and $^{13}C/^{12}C$ of individual cells of the different phenotypes of *C. watsonii*-like cells were measured with the nanoSIMS and used to estimate individual single cell uptake rates for C and N_2 fixation. A summary of the enrichment values and cell-specific uptake rates for C and N_2 fixation is provided in Table 2.

The $^{13}C/^{12}C$ of the colonial and free-living *C. watsonii*-like cells from the initial time point (time 0) was as expected and measured near background (natural abundance, 1.0664 ± 0.0006 ^{13}C atom%) by nanoSIMS (Table 2; Figs. 2, c–d and 3, a–l). Subsequently, both colonial and free-living phenotypes had similar patterns of ^{13}C enrichment where highest average enrichment values (atom%) were measured in cells incubated during the day (Table 2; Figs. 2, c–d and 3, a–b, e–f). The mean ^{13}C enrichment measured in cells of both phenotypes incubated overnight were similarly reduced compared to the previous two time points (Table 2; Figs. 2, c–d and 3, i–j). There were exceptions to these latter observations for the single cell phenotype, but in general, most of the cells were more enriched during the first two time points (3.8 and 12.3 h) than in the overnight incubation.

TABLE 2. Summary of cell diameter measurements and nanoSIMS analysis for *Crocosphaera watsonii*-like cells.

Phenotype	Time (h)	N	Cell diameter (μm)	AT% ^{13}C range (mean ± SE)	C fix rate (fmol C · cell^{-1} · h^{-1}) range (mean ± SE)	C-based growth rate (d^{-1})	AT% ^{15}N range (mean ± SE)	% N_2 fix cells (*n*)	N_2 fix rate [c] (fmol N · cell^{-1} · h^{-1}) range (mean ± SE)
free-living	0	4	3.66–4.61 (4.32 ± 0.22)	1.0352–1.0430 (1.0386 ± 0.0017)	n/a	n/a	0.3674–0.3696 (0.3668 ± 0.0004)	n/a	n/a
free-living dividing[a]	0	6	3.90–4.81 (4.46 ± 0.13)	1.0205–1.0371 (1.0294 ± 0.0069)	n/a	n/a	0.3623–0.3697 (0.3670 ± 0.0011)	n/a	n/a
linear[b]	0	12	3.35–4.14 3.73 ± 0.25)	0.9882–1.0773 (1.0306 ± 0.007)	n/a	n/a	0.3556–0.3707 (0.3643 ± 0.0016)	n/a	n/a
colonial	0	18	6.44–9.55 (8.03 ± 0.16)	1.0205–1.03713 (1.0295 ± 0.0028)	n/a	n/a	0.36223–0.36973 (0.36703 ± 0.0011)	n/a	n/a
free-living	3.8	8	3.77–8.20 (6.46 ± 0.62)	1.0665–1.4264 (1.2861 ± 0.0368)	11.1–120 (70.2 ± 15.2)	0.12–1.68 (1.07 ± 0.16)	0.3542–0.3942 (0.3660 ± 0.0054)	50 (4)	4.44×10^{-3}–0.42 (0.14 ± 0.09)
free-living dividing[a]	3.8	6	6.54–8.65 (7.35 ± 0.36)	1.2989–1.4662 (1.3921 ± 0.0242)	69.8–187 (106 ± 19.2)	1.12–1.85 (1.53 ± 0.10)	0.3431–0.3717 (0.3577 ± 0.0046)	16.7 (1)	0.05
linear[b]	3.8	6	6.84–9.10 (7.51 ± 0.38)	1.3505–1.5719) (1.4342 ± 0.0383)	85.0–247 (126 ± 25.4)	1.35–2.31 (1.71 ± 0.17)	0.3830–0.4198 (0.3973 ± 0.0061)	100 (6)	0.16–0.86 (0.39 ± 0.11)
colonial	3.8	56	4.42–9.69 (6.85 ± 0.16)	1.1379–1.5671 (1.3814 ± 0.0138)	13.9–232 (90.3 ± 7.0)	1.24–2.17 (1.70 ± 0.10)	0.3585–0.4404 (0.3823 ± 0.0028)	88 (49)	2.55×10^{-3}–1.40 (0.26 ± 0.05)
colonial dividing[a]	3.8	12	7.16–12.8 (9.74 ± 0.48)	1.3252–1.5409 (1.4305 ± 0.0221)	125–450 (237 ± 25.8)	0.43–2.29 (1.49 ± 0.06)	0.3632–0.4214 (0.3911 ± 0.0075)	75 (9)	0.03–2.56 (1.09 ± 0.30)
free-living	12.3	11	3.88–6.35 (4.70 ± 0.26)	1.416–1.7392 (1.5590 ± 0.0289)	8.27–23.0 (14.4 ± 1.41)	0.50–0.94 (0.70 ± 0.04)	0.5805–0.9711 (0.7663 ± 0.0455)	100 (11)	0.15–1.19 (0.50 ± 0.12)
free-living dividing[a]	12.3	3	5.81–5.91 (5.86 ± 0.03)	1.3807–1.4613 (1.4157 ± 0.0239)	17.4–20.9 (18.7 ± 1.12)	0.46–0.57 (0.50 ± 0.03)	0.3580–0.3590 (0.3586 ± 0.0003)	0 (0)	n/a
colonial	12.3	68	4.18–8.69 (6.45 ± 0.14)	1.1985–1.7701 (1.5027 ± 0.0186)	4.38–84.3 (34.6 ± 2.72)	0.21–0.98 (0.62 ± 0.02)	0.3501–0.9940 (0.5511 ± 0.0271)	82 (56)	2.10×10^{-3}–2.31 (0.59 ± 0.08)
colonial dividing[a]	12.3	1	9.06	1.4749	66.7	0.58	0.5033	1 (1)	0.81
free-living	18.3	13	3.37–7.38 (4.78 ± 0.39)	1.1076–1.6948 (1.4128 ± 0.0538)	2.16–15.1 (6.43 ± 1.14)	0.06–0.59 (0.34 ± 0.05)	0.4108–2.7010 (1.7325 ± 0.2448)	100 (13)	0.06–1.60 (0.76 ± 0.12)
free-living dividing[a]	18.3	2	5.93–6.49	1.4545–1.4710	14.3–18.8	0.37–0.39	1.6948–1.9877	100 (2)	1.75–2.70
colonial	18.3	93	3.57–8.15 (5.94 ± 0.10)	1.1672–1.6193 (1.3300 ± 0.0100)	2.50–25.9 (10.6 ± 0.55)	0.12–0.52 (0.26 ± 0.02)	0.3765–1.8598 (0.8382 ± 0.0429)	100 (93)	0.01–2.64 (0.66 ± 0.07)
colonial dividing[a]	18.3	2	7.02–9.26	1.2014–1.3865	18.2–18.5	0.15–0.31	0.3841–1.0441	100 (2)	0.08–1.38

[a]cells which were observed connected and/or elongated were considered dividing;
[b]cells of this character were not observed in other time points;
[c]inactive cells were not included in calculating the mean values; n/a, not applicable.

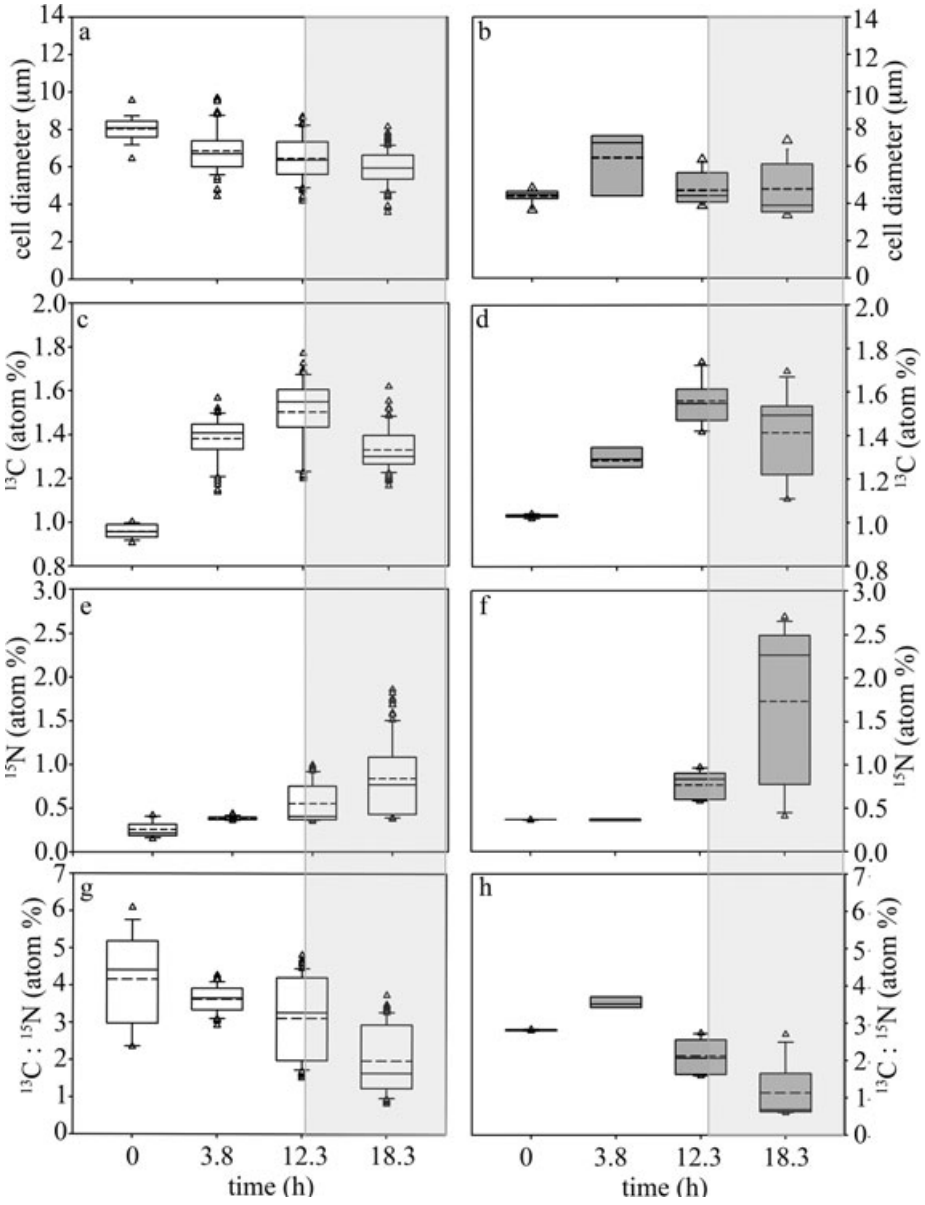

FIG. 2. Summary of phenotypic and nanoSIMS measurements for colonial (left panel: a, c, e and g) and free-living *Crocosphaera watsonii*-like (right panel: b, d, f and h) cells. Box and whisker plots of (a and b) cell diameter, (c and d) $^{13}C/^{12}C$ (atom%), (e and f) $^{15}N/^{14}N$ (atom%), and (g and h) ^{13}C:^{15}N (atom%) for each time point (0, 3.8, 12.3, and 18.3 h). The whiskers represent the 25th and 75th percentile (lower and upper quartiles, respectively) and the mean is shown as a dashed line and median as solid line. Shaded area indicates the dark period.

The highest average C fixation rates in cells of both phenotypes were estimated after the initial 3.8 h of incubation in full sunlight (local time 11:40–15:30; Fig. 4a). The 12 colonial and 6 free-living *C. watsonii*-like cells that were identified as dividing were extremely active for C fixation where the average $^{13}C/^{12}C$ and estimated C fixation rates were higher than their respective nondividing cells (Table 2). The six linear *C. watsonii*-like cells were also highly enriched in ^{13}C (Table 2).

Similar to the $^{13}C/^{12}C$ ratio and as expected for the cells collected from the initial (time 0) time point, *C. watsonii*-like cells were not enriched for $^{15}N/^{14}N$ (Table 2). In contrast to the C enrichment, and as expected for unicellular cyanobacteria which temporally separate N_2 fixation from photosynthesis, not all cells harvested after the 3.8 and 12.3 h time points (day time incubations) were enriched in ^{15}N (Table 2; Figs. 2, e–f and 3, c–d, g–h). For example, the percentage of enriched cells increased with incubation time where 50% and 88% of the free-living and colonial *C. watsonii*-like cells, respectively, were enriched after 3.8 h of sunlight. Subsequently, after an overnight incubation, all cells (100%) of

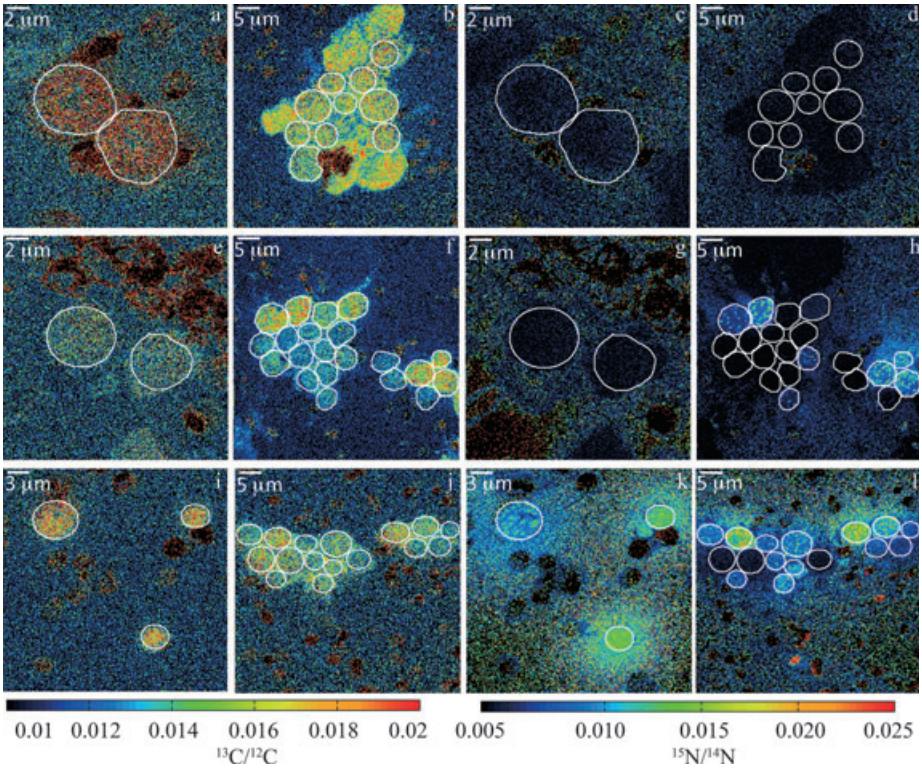

FIG. 3. The nanoSIMS images comparing the isotopic enrichment found in representative single and colonial cells of *Crocosphaera watsonii* after 3.8, 12.3, and 18.3 h of incubation. The $^{13}C/^{12}C$ ratio images are on the left panels (a, b, e, f, i and j) and the $^{15}N/^{14}N$ on the right panels (c, d, g, h, k and l). The incubation of 3.8 (a–d), 12.3 (e–h), and 18.3 (i–l) are shown from top to bottom. The white outlines show regions of interest (ROIs), which were used to estimate the $^{13}C/^{12}C$ and $^{15}N/^{14}N$ ratios.

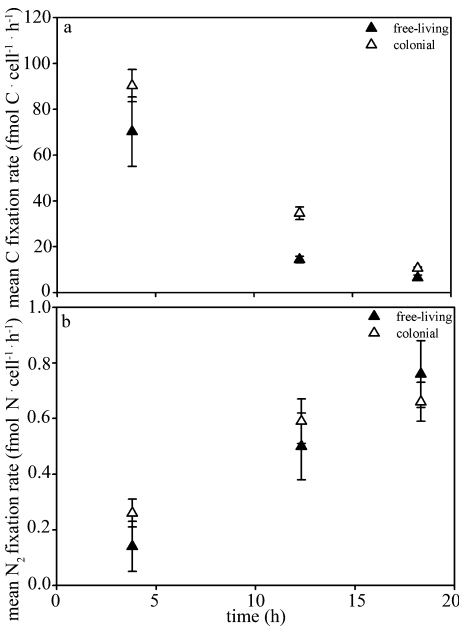

FIG. 4. The average C (a) and N_2 (b) fixation rates as a function of time for both phenotypes. The filled triangles designate the free-living cells, while the open triangles are the colonial *Crocosphaera watsonii*-like cells. Error bars represent the SE.

both phenotypes were enriched for ^{15}N (Table 2; Figs. 2, e–f and 3, k–l). Interestingly, all the *C. watsonii*-like cells observed as a linear phenotype in the first 3.8 h of sunlight were enriched in ^{15}N above background and therefore fixing N_2 or taking up recently fixed N_2 (Table 2).

Although the observations are limited here to the 3.8 h time point, in general, free-living *C. watsonii*-like cells that were in the process of cellular division had reduced $^{15}N/^{14}N$ ratios and a lower percentage of cells actively fixing N_2 (Table 2). On the other hand, the percentage of dividing colonial *C. watsonii*-like cells from the same time point (3.8 h) was actually high for N_2 fixation (75%, 9 of 12 cells) and the highest mean N_2 fixation rate recorded (1.09 ± 0.30 fmol N $\cdot$ cell^{-1} $\cdot$ h^{-1}) was derived from a dividing colonial cell (Table 2).

The $^{15}N/^{14}N$ enrichment ratios were used to determine cell-specific N_2 fixation rates of individual cells (Table 2). The average N_2 fixation rate in both phenotypes and the cell-to-cell variability increased with incubation time (Table 2; Fig 4b). N_2 fixation rates were measurable but low in *C. watsonii*-like cells of both phenotypes during the first 3.8 h daytime incubation. High N_2 fixation rates were estimated after 18.3 h of incubation where the mean rate for *C. watsonii*-like colonial cells was slightly lower (0.66 ± 0.07 fmol N $\cdot$ cell^{-1} $\cdot$ h^{-1}) than the average

for the free-living *C. watsonii*-like cells (0.76 ± 0.12 fmol N · cell^{-1} · h^{-1}; Table 2; Fig. 4b).

The C:N ratios and C-based growth rates were also estimated from the enrichment ratios determined by nanoSIMS (Table 2; Fig. 2, g and h). Both phenotypes had higher average ^{13}C:^{15}N ratio after the initial time point (time 0), and subsequently, ratios declined with incubation time where the decrease in ^{13}C:^{15}N ratio of the free-living cells was strongly negatively correlated ($r^2 = 0.99$). The colonial cells had higher average ^{13}C:^{15}N ratios (Fig. 4, g and h). The average growth rates for both phenotypes were similar and consistently higher in cells measured from the daytime incubation time points. Cell diameter was linearly correlated with growth rate in the colonial *C. watsonii*-like cells from the second incubation time point (12.3 h; $r^2 = 0.53$; Table 2).

Differential ^{15}N and ^{13}C enrichment in colonial C. watsonii*-like cells.* The nanoSIMS imaging made it possible to easily visualize that the $^{15}N/^{14}N$ and $^{13}C/^{12}C$ of cells within a given colony was nonuniform (Fig. S2, a–d, see Supporting Information). In other words, some cells in a given colony were highly enriched in ^{15}N while other cells were apparently inactive for ^{15}N and other cells were active for ^{15}N, but less active for ^{13}C. Furthermore, we estimated that less than 34% of the cells were enriched in both N and C above the mean for the colony (Table S1).

In general, the most active cells for N_2 fixation were located on the periphery of the colony rather than within the interior. In the colonial cells, we also noted small areas (>1 nm) of enriched ^{15}N and ^{13}C resembling storage granules visible in colonial cells at the latter time points (12.3 and 18.3 h; Fig. 3, e–l; Fig. S2, a–d). Similar observations were made for the free-living phenotype; however, it was less frequently observed and limited to cells from the overnight incubation (18.3 h; Fig. 3, i and k).

DISCUSSION

For decades, the imbalanced marine N budget has long been debated and has been a major driver for N_2 fixation research. Large uncertainties of the imbalance are related to the discrepancy of input and loss terms for N (Codispoti 1995, Michaels et al. 1996, Gruber 2005) and whether the full diversity of diazotrophs is fully known (Zehr and Ward 2002). In addition, recent field and laboratory studies have shown that N_2 fixation rate measurements have been quantitatively underestimated by up to 2-fold by standard experimental approaches (Mohr et al. 2010b, Großkopf et al. 2012, Wilson et al. 2012). For the larger filamentous cyanobacteria *Trichodesmium*, colony and filament-based rates are most often reported since individual colonies and filaments can be easily collected and assayed. However, for the smaller cell diameter cells, i.e., unicellular cyanobacteria, there are no direct single cell measurements of N_2 (and C) fixation. Moreover, unicellular cyanobacteria cannot be easily separated from co-occurring cells and the technology to make these types of measurements on single cells was lacking. However, recently, using nanoSIMS, single cell uptake rates are easily accessible and measurable (reviewed in Wagner 2009 and Musat et al. 2011).

The primary objective in this study was to estimate single cell rates of N_2 and C fixation by natural populations using nanoSIMS. Given that unicellular cyanobacteria were one of the dominant populations in our incubation experiments and the recent emphasis on their biogeochemical significance to the N budget (Zehr et al. 2001, Montoya et al. 2004, Moisander et al. 2010), it seemed appropriate to select unicellular diazotrophs as a target population for our single cell analysis. Second, we observed two distinct phenotypes of unicells at the field site, and initially hypothesized that the two cell types (colonial and free-living) could differ in N_2- and C-fixing activity. NanoSIMS imaging provided an ideal approach to measure single cell uptake rates and also revealed subtle differences between the phenotypes, which are not feasible by other more commonly used approaches, i.e., proteomics, bulk isotope ratio mass spectrometry, quantitative molecular assays.

Phenotypic variation in cell diameter of C. watsonii*-like cells.* We identified the unicellular cyanobacteria observed in our incubation bottles based on several morphological and physiological properties characteristic of *C. watsonii* including (i) cell size (ii) cell shape (iii) fluorescence emission signals after excitation with blue and green light filters (iv) excretion of extracellular material (ECM) (v) maximum aerobic N_2 fixation at night and (vi) carbon fixation during the day. Given that the only unicellular cyanobacteria population with the abovementioned characters common at the field site (station ALOHA) is *C. watsonii*, we identified the field populations in our experiments as *C. watsonii*-like cells.

We observed similar abundances for colonial (6.32×10^3 cells · L^{-1}) and free-living (4.78×10^3 cells · L^{-1}) *C. watsonii*-like cells at the start of our incubation experiments. Cells which appeared elongated or in the process of division were also observed early in the experiment, which was consistent with the pattern of increased cell abundances for both the colonial and free-living cells observed at the 3.8 and 12.3 h time points. The observations of dividing cells also suggest that the cells were highly active and growing, and bottle effects common to incubations were minimal.

Previous laboratory studies identify two size classes for *C. watsonii* (2.5–4 μm and 5.0–6 μm), which can differ in N_2 fixation rates, temperature optima, and production of ECM (Falcon et al. 2004, 2005, Webb et al. 2009, Sohm et al. 2011b). The mean cell diameter for the colonial cells was almost twice the mean cell diameter of the free-living cell type at the beginning of the experiment (time 0) and

larger than the cell diameters previously reported for isolated *Crocosphaera* spp. strains (Zehr et al. 2001, 2007b, Falcon et al. 2004, 2005, Webb et al. 2009, Shi et al. 2010). Thus, it seems that *C. watsonii*-like cells are capable of reaching cell diameters more characteristic of the larger size fraction (>10 μm) of N_2 fixers.

The mean cell diameter for the colonial cell type decreased with incubation, while the average cell diameter of the single cell phenotype showed an initial increase and subsequent decrease in mean cell diameter. Cell diameter plasticity has already been observed in some of the *C. watsonii* strains and is a function of temperature where a 14% cell diameter increase was observed in a 3°C temperature shift from 28°C to 25°C (Webb et al. 2009). Potentially, the temperature in the bottle could have changed during the incubation and induced a change in cell morphology; however, the temperature recorded by the HOT time-series shows a stable temperature in the upper 15 m for the 4–5 d occupation at ALOHA. Second, we cannot exclude that the chemical fixation step required for nanoSIMS analysis had an effect on the cell diameter, i.e., shrinkage of cell. However, we would expect the effect to be somewhat uniform after each incubation time point since all cells were treated for the same duration. The reduction in cell diameter could also be attributed to the cell cycle as we did observe many of the cells in the process of cellular division. An important distinction between the colonial and single cell phenotypes that is related to cell diameter in the colonial cells is the synthesis of an ECM in the colonial phenotype.

Extracellular material (ECM) in colonial C. watsonii*-like cells.* Copious amounts of ECM have been reported for 5 of the 10 cultivated strains of *C. watsonii* and typically the strains with ECM have larger cell diameters ($\leq$4.0 μm; Webb et al. 2009). Four of the latter five strains were isolated from the Pacific Ocean and others have made similar observations of field populations of *C. watsonii*-like cells held together in colonies in other regions of the ocean (Campbell et al. 2005, Bonnet et al. 2009, Le Moal and Biegala 2009, Webb et al. 2009). Recently Sohm et al. (2011b) described the ECM of the *C. watsonii* strains as an EPS layer highly enriched in particulate C and depleted in N relative to the cellular C and N. Similarly, we imaged and observed with nanoSIMS, a ^{13}C-enriched and ^{15}N-depleted ECM between the colonial cells, which was absent in the free-living phenotype. The ECM surrounding the colonial cells was also enriched in ^{32}S, which is consistent with observations of S-rich EPS layers in other unicells: *Cyanothece* spp. (De Philippis et al. 1993, 1998, De Philippis and Vincenzini 1998, Pereira et al. 2009) and *Gloethece* spp. (Tease et al. 1991, Pereira et al. 2009).

Sohm et al. (2011b) also showed that the production of EPS was tightly coupled to a higher photochemical efficiency of photosystem II in the larger *C. watsonii* strains. Similarly, in other phytoplankton, EPS production results from the channeling of photosynthetically fixed C into transparent exoplymer particles (TEP) and requires N-limiting conditions (Corzo et al. 2000). The mean C fixation rate of the colonial phenotype was higher than that of the free-living cells. The area between the colonial cells was also highly enriched for ^{13}C at all 3 time points, suggesting that newly fixed C is directly utilized to form the ECM surrounding the colonial cells. The latter observation is consistent with decreases in cellular $^{13}C/^{12}C$ measured in the colonial cells at the latter time points.

Other unicellular diazotrophs, *Cyanothece* and *Gloethece* spp., also excrete ECM in the form of EPS and some suggest that the EPS acts as an adhesive for colony formation and to absorb nutrients (Tease et al. 1991, De Philippis et al. 1993, 1998, De Philippis and Vincenzini 1998, Pereira et al. 2009). There was an increase in the colony size as the incubation progressed. For example, average cell density for a colony in the beginning of the experiment was 17 ± 7 cells $\cdot$ colony^{-1}), and at the later two time points (12.3 and 18.3 h), average cell density was nearly double (37 ± 10 and 33 ± 9 cells $\cdot$ colony^{-1}, respectively). Only the colonial cells were observed with the ECM, and therefore it probably aids in colony formation in the *C. watsonii*-like cells.

Others have found the presence of EPS as a stress response (De Philippis and Vincenzini 1998), or propose the EPS as a strategy to protect the nitrogenase enzyme from oxygen in cyanobacteria (Reddy et al. 1996, Bergman et al. 1997). Interestingly, a higher percentage of the nondividing colonial cells (88%) than single cells (50%) showed enrichment of $^{15}N/^{14}N$ in the first 3.8 h of incubation in the light. Thus, producing ECM could be a strategic mechanism that allows daytime N_2 fixation in *C. watsonii*-like cells.

Single cell N_2 and C fixation rates by C. watsonii*-like cells.* Cyanobacteria are unique to N_2-fixing lineages in that these are the only oxygenic photosynthetic microorganisms capable of N_2 fixation under aerobic conditions. The nitrogenase enzyme necessary for N_2 fixation is inactivated under aerobic conditions, and therefore *C. watsonii* are thought to strictly and temporally separate N_2 fixation from photosynthesis (Compaoré and Stal 2010). Although expression of N_2 fixation genes (*nifH*) shows low transcript abundance in cultured and field populations of *C. watsonii* during day (Church et al. 2005a, b, Mohr et al. 2010a, Pennebaker et al. 2010, Shi et al. 2010, Saito et al. 2011), N_2 fixation rates during the light period by *C. watsonii* have so far not been directly measured. Most N_2 fixation rates reported for *C. watsonii* are from cultured isolates and measured using the acetylene reduction assay, which is an indirect measure of N_2 fixation since acetylene is reduced rather than N_2 (Capone 1993). In addition, most experiments use batch cultures

rather than individual cells. Unexpectedly, we imaged and quantified daytime $^{15}N/^{14}N$ enrichment in the individual *C. watsonii*-like cells. Eighty-eight percent (49 of 56) of the nondividing colonial cells were enriched in ^{15}N above background, and fewer single cells (50%, 4 of 8 cells) were enriched. The enrichment of ^{15}N in the *C. watsonii*-like cells is also surprising given that in culture, *C. watsonii* has been shown to degrade nitrogenase during the day in order to conserve iron for integration into the protein complex that make up the photosynthetic electron transport chain (Saito et al. 2011).

During our experiments, we observed other co-occurring N_2 fixers, i.e., *Trichodesmium* spp. and diatom-*Richelia* symbioses, present in our incubation bottles. These populations are known to reduce N_2 during the day and *Trichodesmium* releases some of their fixed N to the surround (Mulholland et al. 2004). Therefore, we cannot discount that some of the enrichment observed in the *C. watsonii*-like cells was derived in part from a labeled DIN pool.

As can be expected for nighttime N_2 fixers, the number of *C. watsonii*-like cells enriched in ^{15}N increased after the overnight incubation and was consistent in both phenotypes. Our N_2 fixation rate measurements were similar to previously reported rates from culture and field populations estimates (Table 3). However, an important distinction is that field measurements are inferred as the unicellular activity based on size fractionation, whereas, with the nanoSIMS approach, measurements are direct. The higher mean N_2 fixation rates were measured for both phenotypes after 18.3 h of incubation. Other unicellular diazotrophs, including isolate *C. watsonii* 8501, form nonstatic granules composed of protein and carbohydrates during the photoperiod, which are utilized in the dark to support N_2 fixation (Schneegurt et al. 1994, Saito et al. 2011). Similarly, we observed an increase in ^{15}N:^{13}C ratios with incubation time in both phenotypes, suggesting that a percentage of the fixed N and C was stored as protein and/or carbohydrates, and in addition, we observed small "hot spots" of enrichment by the nanoSIMS analysis.

Variability of N_2 and C fixation rates & evidence of diazocytes in colonial C. watsonii*-like cells.* High variability in C and N_2 fixation rates was observed among the cells for a given time point. Although the incubations were short, some of the variation can be attributed to expected bottle effects. In addition, recent evidence shows that $^{15}N_2$ dissolution is nonuniform over the course of an incubation when amended as bubbles resulting in an underestimation that can be linked to the diazotrophic composition (Mohr et al. 2010b, Großkopf et al. 2012, Wilson et al. 2012). Thus, some of our variability, in particular at the later time points, could be related to how the isotope was amended. For example, in general, we noted that the highest ^{15}N of colonial cells was imaged in the cells on the periphery of a colony, which could suggest that the cells in the interior were diffusion limited. However, high variability would also be expected, given differences in observed cell sizes and therefore growth requirements. We also observed significant differences in the measured isotope ratios ($^{15}N/^{14}N$ and $^{13}C/^{12}C$) and cell diameter between the cells identified as in the process of division and those assumed in normal growth phase. Heterogeneity between N_2-fixing bacteria has also been observed and thought to be due to differences in physiological state (Kaern et al. 2005, Chabot et al. 2007, Lechene et al. 2007).

One of the more interesting observations obtained by the nanoSIMS imaging was the division of metabolic activity within a given colony. For example, in the 12.3 and 18.3 h time points, often only a few cells within a colony were highly enriched in ^{15}N, whereas the ^{15}N enrichment in the single cells appeared fairly uniform at each time point. With regard to ^{13}C, all the cells (colonial and single cells) were actively taking up the labeled dissolved inorganic carbon (DIC); however, only 16%–34% of the cells in a colony were enriched in both ^{13}C and ^{15}N above the average. Hence, it seems that partitioning of activity amongst the colonial *C. watsonii*-like cells is similar to the diazocytes of

TABLE 3. Comparative summary of field and cultured rate measurements for *Crocosphaera watsonii*.

N_2 fix rate (fmol N · cell^{-1} · h^{-1})	Field or culture	Experimental Method[a]	Reference
0.12	Field	AR	Falcon et al. (2005)
0.14 ± 0.09	Field	$^{15}N_2$	3.8 h free-living
0.22	Field	$^{15}N_2$	Zehr et al. (2007b)
0.26 ± 0.05	Field	$^{15}N_2$	3.8 h colonial
0.50	Culture	AR	Webb et al. (2009)
0.50 ± 0.12	Field	$^{15}N_2$	12.3 h free-living
0.59 ± 0.08	Field	$^{15}N_2$	12.3 h colonial
0.58	Field	AR	Falcon et al. (2005)
0.59	Culture	AR	Tuit et al. (2004)
0.66 ± 0.07	Field	$^{15}N_2$	18.3 h free-living
0.76 ± 0.12	Field	$^{15}N_2$	18.3 h colonial
6.60	Field	AR	Falcon et al. (2005)
16	Culture	AR	Wilson et al. (2010)

[a] $^{15}N_2$ indicates stable isotope amended incubation experiments where the rate was estimated using the reported cell density or the chlorophyll a content of 1.5×10^{-6} μg chl *a* per cell (Webb et al. 2009) and AR refers to the indirect method of acetylene (C_2H_4) reduction and assumed a 4:1 ratio for C_2H_4:N_2 (Capone 1993).

Trichodesmium, where N_2 fixation is localized to only a few cells of a given filament (Bergman and Carpenter 1991). Similarly, in the colonies of *C. watsonii*-like cells studied here, we often observed only a few of the unicells in a given colony (<34%) highly active for N_2 fixation. We interpreted the highly active cells as the potential diazocytes for the colony. Diazocytes are thought to be strategic and allow daytime N_2 fixation to occur since the nitrogenase can be protected spatially from the oxygen produced during photosynthesis. The induction of diazocytes in *T. erythraeum* IMS 101 is tightly coupled to respiration, degradation of glycogen granules and gas vacuoles, and an elevated expression of genes related to nitrogen metabolism (*ntcA, nifH*), respiration (*coxB2*), and heterocyst differentiation (El- Shehawy et al. 2003, Sandh et al. 2012). In culture, *C. watsonii* 8501 also accumulates and degrades glycogen in accordance with the light cycle (Saito et al. 2011). Although gene transcription was beyond the scope of our study, we did measure decreases in cellular C:N and C fixation rates in the *C. watsonii*-like cells from later time points, indicative of respiratory responses and the development of a reducing environment conducive for N_2 fixation in diazocytes.

C-based growth and storage in C. watsonii*-like cells.* We used the $^{13}C/^{12}C$ ratios to estimate growth rates for the two phenotypes of the *C. watsonii*-like cells. The average growth rates for the single cells and colonial cells were similar (0.34–1.07 d^{-1} and 0.26–1.49 d^{-1}) and comparable to those estimated from cultured isolates of *C. watsonii* (~0.45–0.49 d^{-1}) (Tuit et al. 2004, Goebel et al. 2008). Estimated growth rates in both phenotypes were higher in the earlier time points (3.8 and 12.3 h) than at the latter time point (18.3 h). Observations of cells in the process of division were more frequently noted earlier in the experiment. Furthermore, nanoSIMS imaging showed many colonial cells and a few free-living cells with high $^{15}N/^{14}N$ "hotspots" or storage granules at the later time points. Combined, the latter observations suggest that the cells were more active for growth earlier in the experiment, and probably the N, which was fixed later in the experiment (12.3 and 18.3 h), was stored rather than used for growth.

SUMMARY

Determining the relative importance of microorganisms to biogeochemical cycling has largely been driven by bulk analysis, which is limited, since both the identity of the active organisms and the cell-to cell variability cannot be resolved. A recent model from the same field site studied here (station ALOHA) used field measured cell abundances from qPCR data of *nifH* abundance and derived growth and biomass characteristics to predict a seasonal high in N_2 fixation (51%–97%) by unicellular cyanobacteria (including *C. watsonii* cells) in the winter, while *Trichodesmium* should dominate in the summer (Goebel et al. 2007). However, here using direct measures of N_2 fixation by nanoSIMS measurements on single *C. watsonii*-like cells and direct cell counts by microscopy, we find a significant contribution (24%–63%) to N_2 fixation by *C. watsonii*-like cells during summer at station ALOHA. Incorporating nanoSIMS rate measurements into predictive models is a more direct alternative for predicting N and C cycling, since *nifH* gene abundance (and transcription) is not related to activity, is a relative abundance estimate, and the cell-to-cell variability cannot be resolved.

Initially, we hypothesized that the cells living colonially could have an advantage over the free-living cells to potentially reduce more N_2 or fix N_2 during the day, given the excretion and protection from oxygen by a thick ECM. Although a higher percentage of the colonial cells were enriched in ^{15}N in the first 3.8 h of the daytime incubation, both phenotypes had similar enrichment values ($^{15}N/^{14}N$ ratios) and average N_2 fixation rates, and therefore it remains uncertain if the colonial phenotype has an advantage. Our nanoSIMS imaging clearly showed a partitioning of activity for N_2 and C fixation amongst the colonial cells, which was absent in the free-living cells, and the pattern was reminiscent of a diazocyte. The production of the ECM in the colonial phenotype was also consistent with previous qualitative and quantitative observations as a major reservoir of recently fixed C (Webb et al. 2009, Sohm et al. 2011b).

In conclusion, we show that coexisting field populations of colonial and free-living *C. watsonii*-like cells were consistent with isolated type strains in many phenotypic characters and activities. In addition, we show an unexpected ^{15}N enrichment in the unicells recovered from the daytime, which warrants further experimentation to verify that the cells were actively fixing N_2 or taking up labeled DIN. Others have shown a significant contribution of unicellular cyanobacteria to N_2 fixation; however, these are indirect as they are based on size fractionation (<10 μm) of whole water or measured nighttime activity (Montoya et al. 2004, Biegala and Raimbault 2008, Bonnet et al. 2009). Finally, we show several lines of evidence (morphology, growth, N_2 fixation and C fixation rates) for distinguishing two ecotypes for *C. watsonii*-like cells which, given their distribution, varying life styles (free-living and colonial) and phenotype characteristics (production of ECM), should have different implications for N and C cycling in the upper ocean.

We thank the captains and crew of the *R/V Kilo Moana* and the HOT team from HOT213 in July 2009 for their assistance in the field collections with a special acknowledgment to S. Curless and S. Wilson of University of Hawaii, Manoa. We also want to thank, D. de Beer, D. Franzke, D. Ionescu,

G. Klockgether, G. Lavik, T. Max, N. Musat, A. Ramette, and T. Vagner, for their suggestions, technical support, and advice on data processing and manuscript preparation. At the time of the field experiments, the National Science Foundation (to RAF, BIO OCE 0929015) supported the salary, supplies and field experiments, and the Max Planck Society currently supports the salary of RAF and in addition supported the nanoSIMS and EA-IRMS analyses. Lastly, the authors thank two reviewers for their comments and helpful suggestions.

Bench, S. R., Ilikchyan, I. N., Tripp, H. J. & Zehr, J. P. 2011. Two strains of *Crocosphaera watsonii* with highly conserved genomes are distinguished by strain-specific features. *Front. Aquat. Microbiol.* 2:61. doi:10.3389/fmicb.2011.00261.

Bergman, B. & Carpenter, E. J. 1991. Nitrogenase confined to randomly distributed trichomes in the marine cyanobacterium *Trichodesmium thiebautii*. *J. Phycol.* 27:158–65.

Bergman, B., Gallon, J. R., Rai, A. N. & Stal, L. J. 1997. N_2 Fixation by non-heterocystous cyanobacteria. *FEMS Microbiol. Rev.* 19:139–85.

Berman-Frank, I., Lundgren, P., Chen, Y. B., Kupper, H., Kolber, Z., Bergman, B. & Falkowski, P. 2001. Segregation of nitrogen fixation and oxygenic photosynthesis in the marine cyanobacterium *Trichodesmium*. *Science* 294:1534–7.

Biegala, I. C. & Raimbault, P. 2008. High abundance of diazotrophic picocyanobacteria (<3 μm) in a Southwest Pacific coral lagoon. *Aquat. Microb. Ecol.* 51:45–53.

Bonnet, S., Biegala, I. C., Dutrieux, P., Slemons, L. O. & Capone, D. G. 2009. Nitrogen fixation in the western equatorial Pacific: Rates, diazotrophic cyanobacterial size class distribution, and biogeochemical significance. *Global Biogeochem. Cycles* 23:GB3012.

Burris, R. H. 1991. Nitrogenases. *J. Biol. Chem.* 266:9339–42.

Campbell, L., Carpenter, E. J., Montoya, J. P., Kustka, A. B. & Capone, D. G. 2005. Picoplankton community structure within and outside a *Trichodesmium* bloom in the southwestern Pacific Ocean. *Vie Milieu* 55:185–95.

Capone, D. G. 1993. Determination of nitrogenase activity in aquatic samples using the acetylene reduction procedure. *In* Kemp, P. F., Sherr, B. F., Sherr, E. B. & Cole, J. J. [Eds.] *Handbook of Methods in Aquatic Microbial Ecology*. Lewis Publication, Boca Raton, Florida, pp. 621–631.

Capone, D. G., Zehr, J. P., Paerl, H. W., Bergman, B. & Carpenter, E. J. 1997. *Trichodesmium*, a globally significant marine cyanobacterium. *Science* 276:1221–9.

Capone, D.G., Burns, J., Montoya, J., Subramaniam, A., Mahaffey, C., Gunderson, T., Michaels, T. and Carpenter, E.J. 2005. Nitrogen fixation by Trichodesmium spp.: An important new nitrogen to the tropical and subtropical North Atlantic Ocean. *Global Biogeochem. Cycles 19*. doi: 10.1029/2004 GB00231.

Chabot, J. R., Pedraza, J. M., Luitel, P. & van Oudenaarden, A. 2007. Stochastic gene expression out-of-steady-state in the cyanobacterial circadian clock. *Nature* 450:1249–52.

Church, M. J., Björkman, K. M., Karl, D. M., Saito, M. A. & Zehr, J. P. 2008. Regional distributions of nitrogen-fixing bacteria in the Pacific Ocean. *Limnol. Oceangr.* 53:63–77.

Church, M. J., Jenkins, B. D., Karl, D. M. & Zehr, J. P. 2005b. Vertical distributions of nitrogen-fixing phylotypes at Station ALOHA in the oligotrophic North Pacific Ocean. *Aquat. Microb. Ecol.* 38:3–14.

Church, M. J., Short, C. M., Jenkins, B. D., Karl, D. M. & Zehr, J. P. 2005a. Temporal patterns of nitrogenase gene (*nifH*) expression in the oligotrophic North Pacific Ocean. *Appl. Environ. Microb.* 71:5362–70.

Codispoti, L. 1995. Is the ocean losing fixed nitrogen? *Nature* 376:724.

Compaoré, J. & Stal, L. J. 2010. Oxygen and the light-dark cycle of nitrogenase activity in two unicellular cyanobacteria. *Environ. Microbiol.* 12:54–62.

Corzo, A., Morillo, J. A. & Rodriguez, S. 2000. Production of transparent exopolymer particles (TEP) in cultures of *Chaetoceros calcitrans* under nitrogen limitation. *Aquat. Microb. Ecol.* 23: 63–72.

De Philippis, R., Margheri, M. C., Materassi, R. & Vincenzini, M. 1998. Potential of unicellular cyanobacteria from saline environments as exopolysaccharide producers. *Appl. Environ. Microb.* 64:1130–2.

De Philippis, R., Margheri, M. C., Pelosi, E. & Ventura, S. 1993. Exopolysaccharide production by a unicellular cuanobacterium isolated from a hypersaline habitat. *J. Appl. Phycol.* 5:387–94.

De Philippis, R. & Vincenzini, M. 1998. Exocellular polysaccharides from cyanobacteria and their possible applications. *FEMS Microbiol. Rev.* 22:151–75.

Dore, J. E., Brum, J. R., Tupas, L. M. & Karl, D. M. 2002. Seasonal and interannual variability in sources of nitrogen supporting export in oligotrophic subtropical North Pacific Ocean. *Limnol. Oceangr.* 47:1595–607.

El- Shehawy, R., Lugomela, C., Ernst, A. & Bergman, B. 2003. Diurnal expression of hetR and diazocyte development in the filamentous non-heterocystous cyanobacterium *Trichodesmium erythraeum*. *Microbiology* 149:1139–46.

Falcon, L. I., Carpenter, E. J., Cipriano, F., Bergman, B. & Capone, D. G. 2004. N_2 fixation by unicellular bacterioplankton from the Atlantic and Pacific oceans: Phylogeny and *in-situ* rates. *Appl. Environ. Microb.* 70:765–70.

Falcon, L. I., Pluvinage, S. & Carpenter, E. J. 2005. Growth kinetics of marine unicellular N_2-fixing cyanobacterial isolates in continuous culture in relation to phosphorus and temperature. *Mar. Ecol. Prog. Ser.* 285:3–9.

Fay, P. 1992. Oxygen relations of nitrogen fixation in cyanobacteria. *Microbiol. Rev.* 56:340–73.

Finzi-Hart, J. A., Pett-Ridge, J., Weber, P. K., Popa, R., Fallon, S. J., Gunderson, T., Hutcheon, I. D., Nealson, K. H. & Capone, D. G. 2009. Fixation and fate of C and N in the cyanobacterium *Trichodesmium* using nanometer-scale secondary ion mass spectrometry. *Proc. Natl Acad. Sci. USA* 106:6345–50.

Fong, A. A., Karl, D. M., Lukas, R., Letelier, R. M., Zehr, J. P. & Church, M. J. 2008. Nitrogen fixation in an anticyclonic eddy in the oligotrophic North Pacific Ocean. *ISME J.* 2:663–7.

Foster, R. A., Subramaniam, A., Mahaffey, C., Carpenter, E. J., Capone, D. G. & Zehr, J. P. 2007. Influence of the Amazon River Plume on distributions of free-living and symbiotic cyanobacteria in the Western Tropical North Atlantic Ocean. *Limnol. Oceanogr.* 52:517–32.

Gallon, J. R. & Chaplin, A. E. 1988. Nitrogen fixation. *In* Rogers, L. J. & Gallon, J. R. [Eds.] *The Biochemistry of Algae and Cyanobacteria*. Oxford University Press, Oxford, UK. pp. 147–73.

Goebel, N. L., Edwards, C. A., Carter, B. J., Achilles, K. M. & Zehr, J. P. 2008. Growth and carbon content of three different-sized diazotrophic czanobacteria observed in the subtropical North Pacific. *J. Phycol.* 44:1212–20.

Goebel, N. L., Edwards, C. E., Church, M. J. & Zehr, J. P. 2007. Modeled contributions of three types of diazotrophs to nitrogen fixation at Station ALOHA. *ISME J.* 1:606–19.

Grabowski, M. N. W., Church, M. J. & Karl, D. M. 2008. Nitrogen fixation rates and controls at Stn ALOHA. *Aquat. Micro. Ecol.* 52:175–83.

Griffiths, M. S. H., Gallon, J. R. & Chaplin, A. E. 1987. The diurnal pattern of dinitrogen fixation by cyanobacteria in situ. *New Phytol.* 107:649–57.

Großkopf, T., Mohr, W., Baustian, T., Schunck, H., Gill, D., Kuypers, M. M. M., Lavik, G., Schmitz, R. A., Wallace, D. W. & LaRoche, J. 2012. Doubling of marine dinitrogen-fixation rates based on direct measurements. *Nature* 488:361–4.

Gruber, N. 2005. A bigger nitrogen fix. *Nature* 436:786–7.

Kaern, M., Elston, T. C., Blake, W. J. & Collins, J. J. 2005. Stochasticity in gene expression: From theories to phenotypes. *Nat. Rev. Genet.* 6:451–64.

Karl, D. M., Letelier, R., Tupas, L., Dore, J., Christian, J. & Hebel, D. 1997. The role of nitrogen fixation in biogeochemical cycling in the subtropical North Pacific Ocean. *Nature* 388:533–8.

Karl, D. M., Michaels, A., Bergman, B., Capone, D. G., Carpenter, E. J., Letelier, R., Lipshultz, F., Paerl, H., Sigman, D. & Stal,

L. 2002. Dinitrogen fixation in the world's oceans. *Biogeochemistry* 57/58:47–98.

Kitajima, S., Furuya, K., Hashihama, F., Takeda, S. & Kanda, J. 2009. Latitudinal distribution of diazotrophs and their nitrogen fixation in the tropical and subtropical western North Pacific. *Limnol. Oceangr.* 54:537–47.

Lechene, C. P., Luyten, Y., McMahon, G. & Distel, D. L. 2007. Quantitative imaging of nitrogen fixation by individual bacteria within animal cells. *Science* 317:1563–6.

Le Moal, M. & Biegala, I. 2009. Diazotrophic unicellular cyanobacteria in the northwestern Mediterranean Sea: a seasonal cycle. *Limnol. Oceanogr.* 54:845–55.

Leteliar, R. M. & Karl, D. M. 1996. The role of Trichodesmium spp. in the productivity of the subtropical North Pacific Ocean. *Mar. Ecol. Prog. Ser.* 133:263–73.

Lundgren, P., Söderbäck, E., Singer, A., Carpenter, E. J. & Bergman, B. 2001. *Katagnymene:* characterization of a novel marine diazotroph. *J. Phycol.* 37:1052–62.

Mague, T., Weare, N. & Holm-Hansen, O. 1974. Nitrogen fixation in the North Pacific Ocean. *Mar. Biol.* 24:109–19.

Michaels, A., Olson, D., Sarmiento, J., Ammerman, J., Fanning, K., Jahnke, R., Knap, A. H., Lipschultz, F. & Prospero, J. M. 1996. Inputs, losses and transformations of nitrogen and phosphorus in the pelagic North Atlantic Ocean. *Biogeochemistry* 35:181–226.

Mohr, W., Großkopf, T., Wallace, D. R. W. & LaRoche, J. 2010b. Methodological underestimation of oceanic nitrogen fixation rates. *PLoS ONE* 9:1–7.

Mohr, W., Intermaggio, M. P. & LaRoche, J. 2010a. Diel rhythm of nitrogen and carbon metabolism in the unicellular, diazotrophic cyanobacterium *Crocosphaera watsonii* WH8501. *Environ. Microbiol.* 12:412–21.

Moisander, P. H., Beinart, R. A., Hewson, I., White, A. E., Johnson, K. S., Carlson, C. A., Montoya, J. P. & Zehr, J. P. 2010. Unicellular cyanobacterial distributions broaden the oceanic N_2 fixation domain. *Science* 327:1512–4.

Monteiro, F., Follows, M. J. & Dutkiewicz, S. 2010. Distribution of diverse nitrogen fixers in the global ocean. *Global Biogeochem. Cy.* 24:GB3017. doi: 10.1029/2009GB003731

Montoya, J. P., Holl, C. M., Zehr, J. P., Hansen, A., Villareal, T. A. & Capone, D. G. 2004. High rates of N_2 fixation by unicellular diazotrophs in the oligotrophic Pacific Ocean. *Nature* 430:1027–31.

Montoya, J. P., Voss, M., Kahler, P. & Capone, D. G. 1996. A simple, high-precision, high-sensitivity tracer assay for N_2 fixation. *Appl. Environ. Microb.* 62:986–93.

Mulholland, M., Bronk, D. A. & Capone, D. G. 2004. Dinitrogen fixation and release of ammonium and dissolved organic nitrogen by *Trichodesmium* IMS 101. *Aquat. Microb. Ecol.* 37: 85–94.

Musat, M., Foster, R. A., Vagner, T., Adam, B. A. & Kuypers, M. M. M. 2011. Detecting metabolic activities in single cells, with emphasis on nanoSIMS. *FEMS Microbiol. Rev.* 36:486–511.

Needoba, J. A., Foster, R. A., Sakamoto, C., Zehr, J. P. & Johnson, K. S. 2007. Nitrogen fixation by unicellular diazotrophic cyanobacteria in the temperate North Pacific Ocean. *Limnol. Oceangr.* 52:1317–27.

Pennebaker, K., Mackey, K. R. M., Smith, R. M., Williams, S. B. & Zehr, J. P. 2010. Diel cycling of DNA staining and *nifH* gene regulation in the unicellular cyanobacterium *Crocosphaera watsonii* strain WH 8501 (Cyanophyta). *Environ. Microbiol.* 12:1001–10.

Pereira, S., Zille, A., Micheletti, E., Moradas-Ferreira, P., De Philippis, R. & Tamagnini, P. 2009. Complexity of cyanobacterial exopolysaccharides: composition, structures, inducing factors and putative genes involved in their biosynthesis and assembly. *FEMS Microbiol. Rev.* 33:917–41.

Polerecky, L., Adam, B., Milucka, J., Musat, N., Vagner, T. & Kuypers, M. M. M. 2012. Look@NanoSIMS – a tool for the analysis of nanoSIMS data in environmental microbiology. *Environ. Microbiol.* 4:1009–23.

Postgate, J. 1998. *Nitrogen Fixation, 3rd ed.* Cambridge University Press, Cambridge, United Kingdom, 61 pp.

Reddy, K. J., Soper, B. W., Tang, J. & Bradley, R. L. 1996. Phenotypic variation in exopolysaccharide production in the marine, aerobic nitrogen-fixing unicellular cyanobacterium *Cyanothece* sp. *World. J. Microb. Biot.* 12:311–8.

Saito, M. A., Bertrand, E. M., Dutkiewicz, S., Bulygin, V. V., Moran, D. M., Monteiro, F. M., Follows, M. J., Valois, F. W. & Waterbury, J. B. 2011. Iron conservation by reduction of metalloenzyme inventories in the marine diazotroph *Crocosphaera watsonii*. *Proc. Natl Acad. Sci. USA* 108:2184–9.

Sandh, G., Xu, L. & Bergman, B. 2012. Diazocyte development in the marine diazotrophic cyanobacterium *Trichodesmium*. *Microbiology* 158:345–52.

Schneegurt, M. A., Sherman, D. M., Nayer, S. & Sherman, L. A. 1994. Oscillating behavior of carbohydrate granule formation and dinitrogen fixation in the cyanobacterium *Cyanothece* sp. strain ATCC51142. *J. Bacteriol.* 176:1586–97.

Shi, T., Ilikchyan, I., Rabouille, S. & Zehr, J. P. 2010. Genome-wide analysis of diel gene expression in the unicellular N_2-fixing cyanobacterium *Crocosphaera watsonii* WH 8501. *ISME J.* 4:621–32.

Sohm, J.A., Edwards, B.R., Wilson, B.G. & Webb, E.A. 2011b. Constitutive extracellular polysaccharide (EPS) production by specific isolates of *Crocosphaera watsonii*. *Frontiers in Microbiol.* 2:1–9. Doi. 10.3389/fmicb.2011.00229.

Sohm, J. A., Subramaniam, A., Gunderson, T. E., Carpenter, E. J. & Capone, D. G. 2011a. Nitrogen fixation by Trichodesmium and unicellular diazotrophs in the North Pacific Subtropical Gyre. *Journal Geophys. Res.* 116:1–12.

Sun, J. & Liu, D. Y. 2003. Geometric models for calculating cell biovolume and surface area for phytoplankton. *J. Plankton Res.* 25:1331–46.

Tease, B., Jurgens, U. J., Golecki, J. R., Heinrich, U. R., Rippka, R. & Weckesser, J. 1991. Fine-structural and chemical-analyses on inner and outer sheath of the cyanobacterium *Gloeothece* sp. PCC-6909. *Anton. Leeuw. Int. J. G.* 59:27–34.

Tuit, C., Waterbury, J. & Ravizzaz, G. 2004. Diel variation of molybdenum and iron in marine diazotrophic cyanobacteria. *Limnol. Oceanogr.* 49:978–90.

Verity, P. G., Robertson, C. Y., Tronzo, C. R., Andrews, M. G., Nelson, J. R. & Sieracki, M. E. 1992. Relationships between cell volume and the carbon and nitrogen content of marine photosynthetic nanoplankton. *Limnol. Oceanogr.* 37:1434–46.

Wagner, M. 2009. Single-cell ecophysiology of microbes as revealed by raman microspectroscopy or secondary ion mass spectrometry imaging. *Ann. Rev. Microbiol.* 63:411–29.

Waterbury, J. B. & Rippka, R. 1989. The order Chroococcales. In Krieg, N.R. and Holt, J. B. [Ed.] *Bergey's Manual of Systematic Bacteriology*. Vol. 3. Williams & Wilkens Baltimore, MD, USA, pp. 1728–1746.

Webb, E. A., Ehrenreich, I. M., Brown, S. L., Valois, F. W. & Waterbury, J. B. 2009. Phenotypic and genotypic characterization of multiple strains of the diazotrophic cyanobacterium, *Crocosphaera watsonii*, isolated from the open ocean. *Environ. Microbiol.* 11:338–48.

Wilson, S. T., Böttjer, D., Church, M. J. & Karl, D. M. 2012. Comparative assessment of nitrogen fixation methodologies conducted in the oligotrophic North Pacific Ocean. *Appl. Envir. Microbiol.* 78:6516–23.

Wilson, S. T., Foster, R. A., Zehr, J. P. & Karl, D. M. 2010. Hydrogen production by *Trichodesmium erythraeum*, *Cyanothece* sp. and *Crocosphaera watsonii*. *Aquat. Microb. Ecol.* 59:197–206.

Wolk, C. P., Thomas, J., Shaffer, P. W., Austin, S. M. & Galonsky, A. 1976. Pathway of nitrogen metabolism after fixation of ^{13}N-labeled nitrogen gas by the cyanobacterium *Anabaena cylindrical*. *J. Biol. Chem.* 251:5027–34.

Zehr, J. P., Bench, S. R., Mondragon, E. A., McCarren, J. & DeLong, E. F. 2007b. Low genomic diversity in tropical oceanic N_2-fixing cyanobacteria. *Proc. Natl. Acad. Sci.* USA 104:17807–12.

Zehr, J. P., Mellon, M. T. & Zani, S. 1998. New nitrogen-fixing microorganisms detected in oligotrophic oceans by amplification of nitrogenase (*nifH*) genes. *Appl. Environ. Microbiol.* 64:3444–50.

Zehr, J. P., Montoya, J. P., Hewson, I., Mondragon, E., Short, C. M., Hansen, A., Jenkins, B. D., Church, M. J. & Karl, D. M. 2007a. Experiments linking nitrogenase gene expression to nitrogen fixation in the North Pacific subtropical gyre. *Limnol. Oceanogr.* 52:169–83.

Zehr, J. P. & Ward, B. B. 2002. Nitrogen cycling in the ocean: New perspectives on processes and paradigms. *Appl. Environ. Microbiol.* 68:1015–24.

Zehr, J. P., Waterbury, J. B., Turner, P. J., Montoya, J. P., Omoregie, E., Steward, G. F., Hansen, A. & Karl, D. M. 2001. Unicellular cyanobacteria fix N_2 in the subtropical North Pacific Ocean. *Nature* 412:635–8.

Supporting Information

Additional Supporting Information may be found in the online version of this article at the publisher's web site:

Table S1. Summary of the average percentage of colonial *Crocosphaera watsonii*-like cells (± standard error) in a given colony with higher ^{15}N, ^{13}C, or both ^{15}N and ^{13}C enrichment than the mean for the colony. The mean number of cells per colony is also provided.

Figure S1. NanoSIMS imaging of the ^{32}S (a) and $^{32}S/^{12}C$ (b) ratio in the colonial *Crocosphaera watsonii*-like cells. Scale bar is 5 μm.

Figure S2. NanoSIMS imaging of colonial *Crocosphaera watsonii*-like cells shows evidence for diazocytes. (a-b) the $^{13}C/^{12}C$ and the $^{15}N/^{14}N$ of a colony from 12.3 h of incubation. (c-d) the $^{13}C/^{12}C$ and the $^{15}N/^{14}N$ of a colony from 18.3 h of incubation. Note in the $^{15}N/^{14}N$ images small localized areas of high enrichment similar in size expected of storage granules. Scale bar is 5 μm.